

SMALL-SCALE TESTING ON GROUND SHOCK PROPAGATION IN MIXED GEOLOGICAL MEDIA

Yingxin ZHOU and Karen O Y CHONG

Lands & Estates Organization, Ministry of Defense, 1 Depot Road #12-05, Singapore 109679.
Phone: +65 373-3570. Fax: +65 273-5754.

Yaokun WU, Singapore Technologies Construction Pte Ltd, 9 Bishan Place #08-00, Singapore 579837, Tel: +65 5528381. Fax: +65 5523780.

ABSTRACT

This paper presents results of a series of small-scale tests conducted to investigate shock propagation through mixed geological media. The tests were conducted in a granite quarry pit. Soil backfill with geotechnical properties similar to the *in situ* residual soil was placed on top of the granite rock to simulate the soil cover. A vertical charge hole was drilled in the granite rock to simulate an underground storage chamber. Various types of gauges were placed in rock boreholes as well as in the soil backfill. For the soil backfill, gauges were placed along the soil/rock boundary, at mid-height, and on the surface of the soil, all at the same horizontal distances. A total of eight charges were detonated to study the effects of coupling, chamber loading density, charge shape and location, and the effect of water.

Results from these tests have provided valuable data for calibration of generic computer models developed for the prediction of ground shock propagation, and contributed significantly to the understanding of shock wave propagation through mixed geological media.

INTRODUCTION

In explosives safety, the inhabited building distance, or IBD, for an accidental underground explosion is based on two parameters. The first is the ground motion generated by the explosion at a given distance. The second is the allowable ground motions for residential buildings. Thus, prediction of ground shock in geological media is a very important step.

The current codes are based on the assumption that the potential explosion site (PES) and exposed site (ES) are in the same geological media in order to apply the criteria for ground shock. Thus, it is not adequate for the unique geology of a hard bed rock overlain by a thick soil layer such as the granite formation in Singapore. In this mixed media, the most likely scenario is a PES sited in hard rock and an ES in soil layer. In such cases, prediction of ground shock is much more complicated and there is very little data in the literature that addresses this problem.

Report Documentation Page			<i>Form Approved OMB No. 0704-0188</i>	
<p>Public reporting burden for the collection of information is estimated to average 1 hour per response, including the time for reviewing instructions, searching existing data sources, gathering and maintaining the data needed, and completing and reviewing the collection of information. Send comments regarding this burden estimate or any other aspect of this collection of information, including suggestions for reducing this burden, to Washington Headquarters Services, Directorate for Information Operations and Reports, 1215 Jefferson Davis Highway, Suite 1204, Arlington VA 22202-4302. Respondents should be aware that notwithstanding any other provision of law, no person shall be subject to a penalty for failing to comply with a collection of information if it does not display a currently valid OMB control number.</p>				
1. REPORT DATE AUG 1998	2. REPORT TYPE	3. DATES COVERED 00-00-1998 to 00-00-1998		
4. TITLE AND SUBTITLE Small-Scale Testing on Ground Shock Propagation in Mixed Geological Media				
5a. CONTRACT NUMBER				
5b. GRANT NUMBER				
5c. PROGRAM ELEMENT NUMBER				
6. AUTHOR(S)				
5d. PROJECT NUMBER				
5e. TASK NUMBER				
5f. WORK UNIT NUMBER				
7. PERFORMING ORGANIZATION NAME(S) AND ADDRESS(ES) Ministry of Defense,Lands & Estates Organization,1 Depot Road #12-05,Singapore 109679,				
8. PERFORMING ORGANIZATION REPORT NUMBER				
9. SPONSORING/MONITORING AGENCY NAME(S) AND ADDRESS(ES)				
10. SPONSOR/MONITOR'S ACRONYM(S)				
11. SPONSOR/MONITOR'S REPORT NUMBER(S)				
12. DISTRIBUTION/AVAILABILITY STATEMENT Approved for public release; distribution unlimited				
13. SUPPLEMENTARY NOTES See also ADM001002. Proceedings of the Twenty-Eighth DoD Explosives Safety Seminar Held in Orlando, FL on 18-20 August 1998.				
14. ABSTRACT see report				
15. SUBJECT TERMS				
16. SECURITY CLASSIFICATION OF:			17. LIMITATION OF ABSTRACT Same as Report (SAR)	18. NUMBER OF PAGES 11
a. REPORT unclassified	b. ABSTRACT unclassified	c. THIS PAGE unclassified	19a. NAME OF RESPONSIBLE PERSON	

TEST SETUP

Site Geology

The geology of the rock formation of the site is a medium-grained granite bedrock, overlain by a residual soil. The soil cover ranges from a few meters to 60 m, with an average thickness of about 15-20 meters. The test site is located in the pit of a granite quarry.

The rock mass is generally considered good to very good, with an average seismic velocity of 5820 m/sec, a density of 2,650 kg/m³, and a uniaxial compressive strength of 150-200 MPa. Geological investigations indicate four major and two minor joint sets, with the pre-dominant sets being sub-vertical and an average joint spacing of 0.39 – 0.62 m. The joints are generally sight and often sealed by calcite. Ground water is about one meter below surface.

Test Layout

Figures 1 and 2 show the test layout. The layout consisted of a vertical charge hole, five gauge holes in the rock, and a soil backfill meant to simulate the soil cover. The vertical charge hole is used to simulate an underground storage chamber. It is 14 meters deep, with the top 6 m for containment, the middle 5 m as the charge chamber, and the lower 3 m for the calibration charge (filled up after the calibration test). The charge chamber has an average diameter of 0.8 m. A steel frame of 6 m long with a concrete plug and concrete weights was used to contain the explosion effects. An airblast gauge was also installed at the end of the plug to measure the internal blast pressure of the charge chamber.

The five vertical holes were used to install motion gauges in rock at charge levels for measurements of free-field motions. Gauges were placed at 2.5 m, 5 m, 10 m, 25 m, and 50 m from the center of charge. In all five holes, gauges were placed at 8.5 m (charge chamber center) and along the surface. Three holes also have gauges installed 14-m depth for measurements of the calibration shot, which was located at the bottom of the charge hole.

The soil backfill of 1.5 m thick is in the opposite direction and symmetric to the charge hole. It is a quarter-circular shape extending from the charge hole with a radius of 60 meters. The extra 10 m beyond the last gauges was to eliminate interaction of reflected waves from the boundary. Gauges were installed at the surface level, mid depth level, and at the soil/rock interface. To simulate the response of steel utility pipelines, a steel pipe with was buried at mid depth in the soil.

Explosives Charge and Test Design

A total of eight tests were conducted. The explosives used for all eight tests were made of plastic PTN explosives with about 20% wax with equivalent TNT of 1.088. **Table 1** shows a summary of the explosives charge amount and objectives of each test.

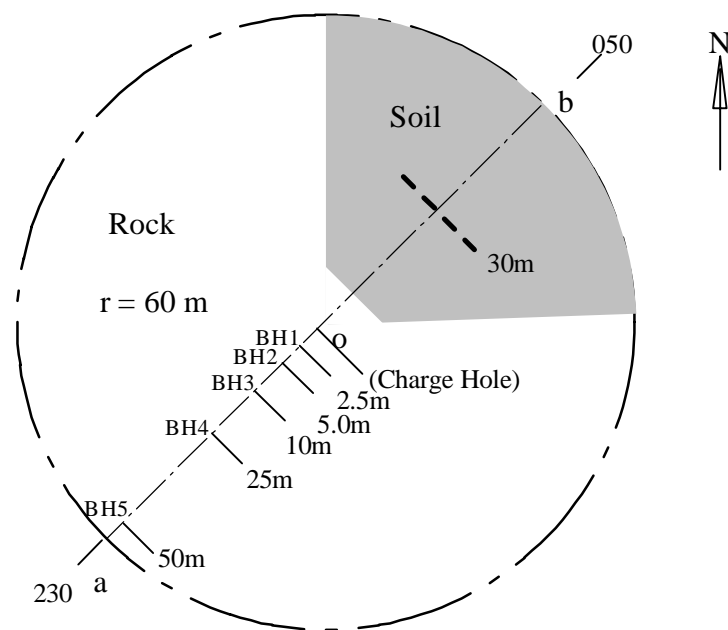


Figure 1. Test site layout at the Mandai Quarry

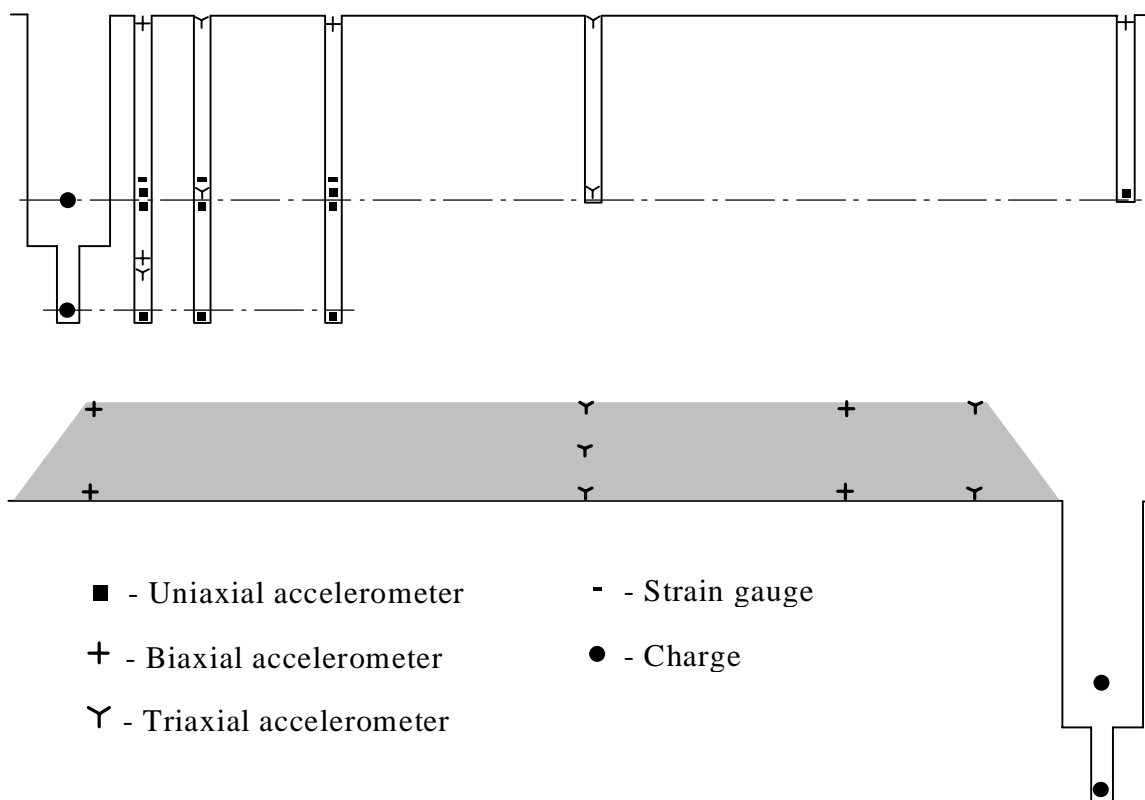


Figure 2. Sensor arrangement along oa and ob (not to scale)

Test #1 was a fully coupled calibration test detonated at the bottom hole. Tests #2, 3, 4, and 8 were basic tests with the charge placed at the center of the chamber. Test #5 was for contact effects while Test #6 was for shape effects. In Test #7, the charge was fully submerged in water.

Table 1. Summary of explosive charge and test objectives

Test No.	Planned charge weight (kg)	Actual charge weight (kg)	L. D. (kg/m ³)	Location of explosive	Purpose
1	25	27.2	fully coupled	calibration hole	fully coupled calibration
2	2.5	2.74	1	center of charge chamber	effect of loading density
3	12.5	8.6	5	center of charge chamber	effect of loading density
4	25	16.3	10	center of charge chamber	effect of loading density
5	25	18.7	10	Line OA side, mid-height of charge chamber	effect of side contact
6	25	19.3	10	sphere charge at center of charge chamber	effect of spherical charge
7	25	19.3	10	center of charge chamber	effect of water coupling
8	50	41.5	20	center of charge chamber	effect of loading density

During the test, loose and damaged rocks fell off the chamber wall and the volume of the chamber was changed slightly. The charge weight was therefore adjusted after each test to keep the planned loading density.

With the exception of Test #1 (coupled) and #5 (spherical), the charge for each test was molded into a cylinder having a 1:6 diameter-to-length ratio and placed on a wooden stand. In order to minimize the influence of seeping ground water, water pumps were running continually before detonation time.

Instrumentation

A total of 55 gauges were installed, with 35 accelerometers (13 triaxial, 13 bi-axial, and 9 uniaxial), 10 bi-axial pressure meters, and 10 uniaxial strain gauges. The total number of signal channels was 75. In addition, two pieces of LQ pressure meters were set up on the soil surface at distances of 10 m and 25 m, respectively, to monitor pressure of the airblast leaked from the charge hole. Gauges installed in rock were mounted in metal canisters and grouted in the gauge holes with a metallic grout called Masterflow 880. The grout is a non-shrink iron reinforced grouting material with high early and ultimate strength (70 MPa at 28 days). Data recording was

done using one 24-channel digital recorder and three 24-channel analogue recorders. Data recorded on the analogue recorder were transferred to the digital recorder immediate after each test for preliminary data processing using a software called DPLOT developed at the Waterways Experiment Station.

TEST RESULTS

A total of more than 500 signals were recorded. Generally, the tests achieved their planned objectives. Regression analyses have established empirical relationships between accelerations and peak particle velocities and scaled range for motions in rock free field, on the rock surface, along the soil/rock interface, and on soil surface. **Table 2** shows a summary of the established equations. The following presents a discussion of the results.

Table 2. Summary of ground shock equations on different surfaces

Location	Accelerations	
In rock free field	$A = 1928.2 (R / Q^{1/3})^{-1.4531}$	r=0.9617
On rock surface	$A_x * (R_v / Q^{1/3}) = 9.8138e^{-0.1245(Rh/Q^{0.333})}$	r=0.9217
	$A_z * (R_v / Q^{1/3}) = 42.6 (R_h / Q^{1/3})^{-1.0912}$	r=0.8189
On interface	$A_x * (R_v / Q^{1/3}) = 4.872e^{-0.0902(Rh/Q^{0.333})}$	r=0.9006
	$A_z * (R_v / Q^{1/3}) = 38.391 (R_h / Q^{1/3})^{-1.3183}$	r=0.9558
On soil surface	$A_x * (R_v / Q^{1/3}) = 2.7744e^{-0.0663(Rh/Q^{0.333})}$	r=0.8088
	$A_z * (R_v / Q^{1/3}) = 37.897 (R_h / Q^{1/3})^{-1.5204}$	r=0.8969
Location	Peak particle velocities	
In rock free field	$PPV = 395.76 (R / Q^{1/3})^{-1.1455}$	r=0.9708
On rock surface	$PPV_x * (R_v / Q^{1/3}) = 118.89e^{-0.1245(Rh/Q^{0.333})}$	r=0.8764
	$PPV_z * (R_v / Q^{1/3}) = 277.07 (R_h / Q^{1/3})^{-1.134}$	r=0.9027
On interface	$PPV_x * (R_v / Q^{1/3}) = 155.2e^{-0.1447(Rh/Q^{0.333})}$	r=0.9078
	$PPV_z * (R_v / Q^{1/3}) = 340.02 (R_h / Q^{1/3})^{-0.8945}$	r=0.8579
On soil surface	$PPV_x * (R_v / Q^{1/3}) = 53.089e^{-0.122(Rh/Q^{0.333})}$	r=0.9509
	$PPV_z * (R_v / Q^{1/3}) = 969.53 (R_h / Q^{1/3})^{-1.8801}$	r=0.899

Ground Shock Propagation in Free Field

When the peak particle velocity is used in computing the IBD, it is generally assumed that the free field velocity will be used. Thus, it is of interest to measure free field wave propagation. Free-field motions are also used as references because they are not affected by other complex wave forms such as those from reflection and refraction.

Based on the data obtained, the following ground shock attenuation equations in rock free field can be obtained for acceleration and peak particle velocity (radial), respectively:

$$A = 1928.2 \left(\frac{R}{Q^{1/3}} \right)^{-1.45}$$

$$V = 396 \left(\frac{R}{Q^{1/3}} \right)^{-1.15}$$

Where A = g, V = mm/sec, R = meters, Q = kg.

Figure 3 shows a comparison of peak particle velocities with measurements by WES in hard limestone. As can be seen, the measurements in granite show a slower attenuation rate than those by WES. There are two possible reasons. First, the porosity of limestone is generally much higher than that of granite. Second, the scale of the tests in granite is much smaller with a maximum charge weight of 43 kg, compared to 3500 kg in tests done by WES. Based on numerous data from other blasting operations, larger scale tests generally show a faster attenuation rate (Dowding, 1996). Rock material tends to exhibit more elastic behavior under smaller loading and at larger scaled ranges.

Effects of Soil Cover

Figures 4 and 5 show a comparison of horizontal ground motions in free field rock, on rock surface, along the soil/rock interface, as well as along the soil surface.

The attenuation effects of the soil cover on horizontal motions are evident. The trend of attenuation for the rock surface and soil surface is also typical of theoretical calculations.

The peak horizontal and vertical motions along the soil surface and soil/rock interface also show distinctively different patterns of attenuation within the scaled range of data. Generally, soil effects are more pronounced for accelerations than for peak particle velocities, and for motions in the horizontal direction than in the vertical direction.

It is important to note that at near field, the vertical peak particle velocities are actually higher than the rock free-field ppv at the same range. This is due to the amplifying effects when the

shock wave crosses the soil/rock interface at near normal angle, and the stronger reflection from the free surface.

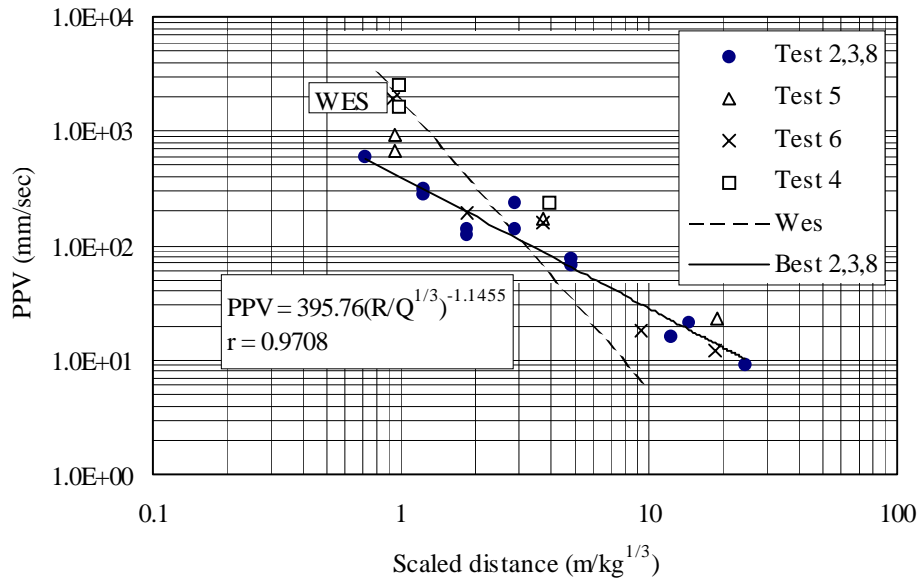


Figure 3. Wave propagation in rock free field

Calibration of Computer Modeling

The test data have been used to calibrate computer modeling using AUTODYN with modified material models for the granite rock based on an equivalent continuum model for rock mass which takes into account rock constitutive relations, strength and failure characteristics, as well as strain rate effect.

Two based tests (#3 and #8) were calculated. For Test #8 (loading density of 20 kg/m³), plastic flow and damage zone is established around the charge chamber, while for Test #3 (loading density of 5 kg/m³) the rock remains elastic because the pressure induced is still small. This is consistent with previous studies carried out in modeling airblast propagation, in which it was shown that at loading densities greater than 5 kg/m³, ground shock effects must be taken into account.

OTHER OBSERVATIONS

Rock Mass Damage

As the tests were conducted in the same charge hole, there was concern about the effects of rock damage on shock wave propagation. In order to address this concern, the arrival time of the shock wave was monitored during each test. These arrival times were then used to calculate the

seismic velocities. **Figure 6** shows a comparison of the arrival times versus distances for six tests. All six lines show the similar slopes, with an estimated seismic velocity of 5838 m/sec, compared to 5820 m/s from seismic surveys. Thus, it was concluded that at the range of measurements, the propagation velocities of the rock were not altered by blast. Subsequent numerical analysis of rock damage and geophysical survey of the charge hole indicated a final damage radius of less than 1.5 meters.

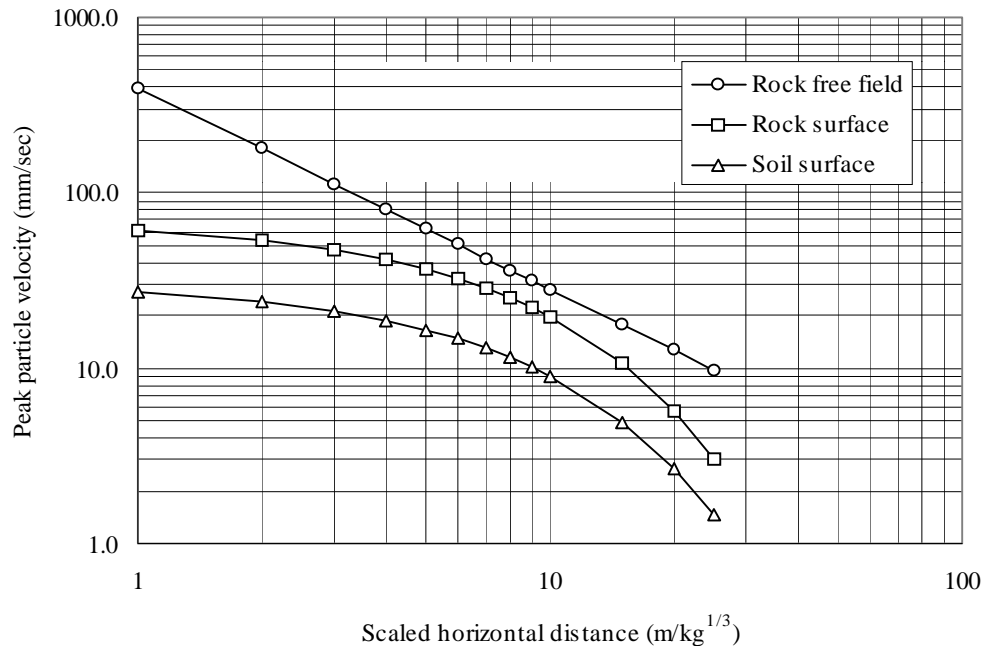


Figure 4. Comparison of horizontal peak particle velocities

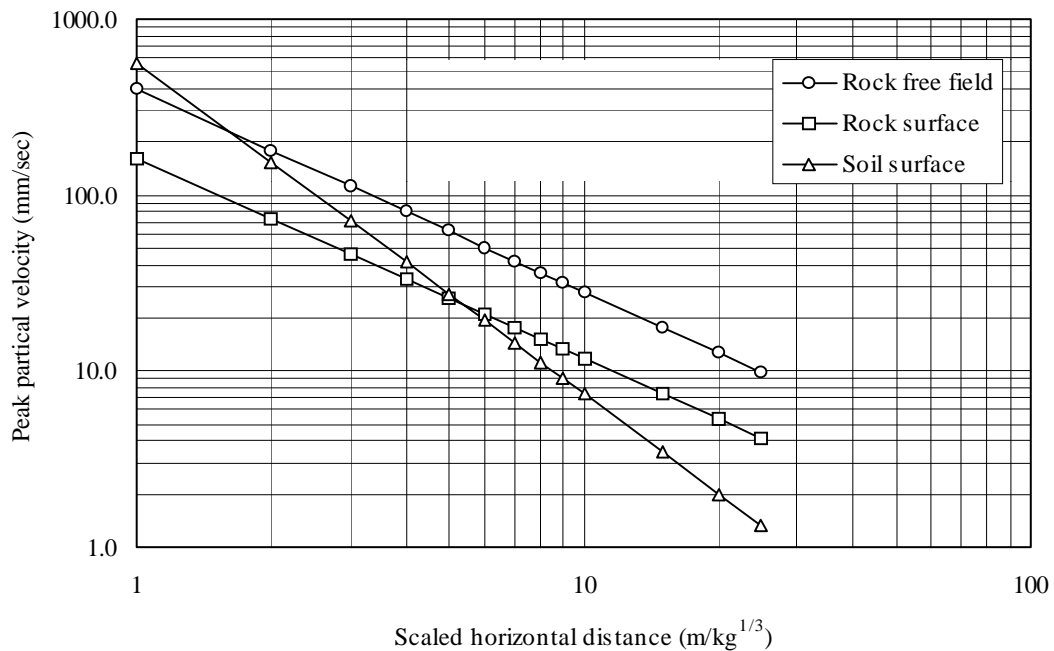


Figure 5. Comparison of vertical peak particle velocities

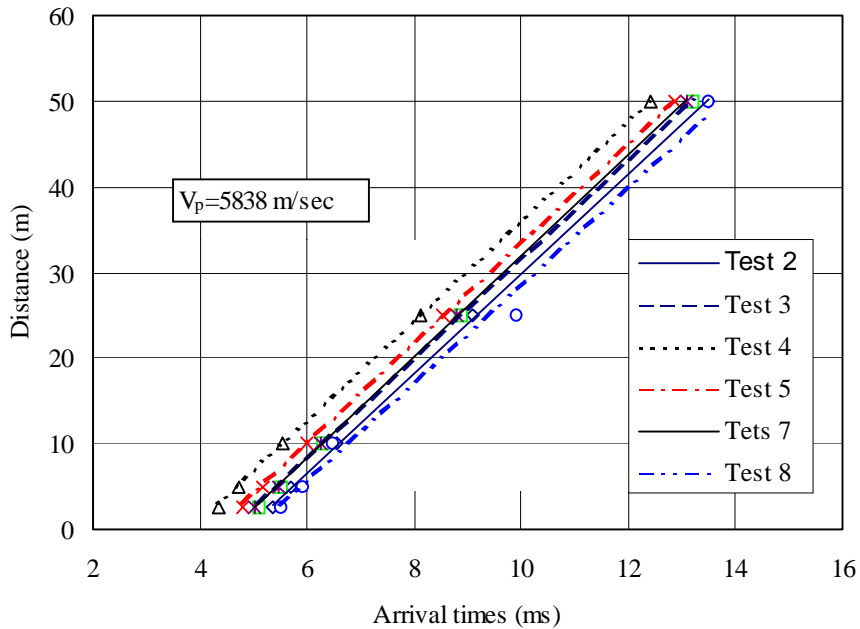


Figure 6. Arrival times versus distances

Effects of Joint Orientation

To study the effects of joint orientation on ground shock propagation, accelerators were also set up on the rock surface along three lines at 0°, 45°, and 90° with respect to the strike of the predominant joint sets (Wu et al., 1998).

Figure 7 shows the peak accelerations versus the angles with respect to the joint strike. Figure 8 shows the power spectrum of shock waves recorded at different incident angles. The accelerations were normalized for three tests where such measurements were made. The data were in good agreement with theoretical analysis of wave propagation, with the amplitude and frequency of the shock wave decreasing rapidly with the increased angle between wave propagation path and joint strike.

Effect Tests

Other tests designed to test the effects of charge shape and location also showed some interesting results. Test #5, where the charge was placed in contact with the chamber wall, produced peak accelerations and peak particle velocities about twice as high as the basic tests. Higher ground motions in near field were also recorded for Test#6, in which the charge was a concentrated spherical shape. However, the effects tend to diminish with increased distance. For the purpose of design, these effects are not sufficiently significant and therefore can be ignored. For Test#7, the charge was submerged in water. Ground motions recorded for this test were similar to those of

the coupled charge, showing the coupling effect of water when in contact with the chamber wall. However, airblast recorded on the surface was much reduced.

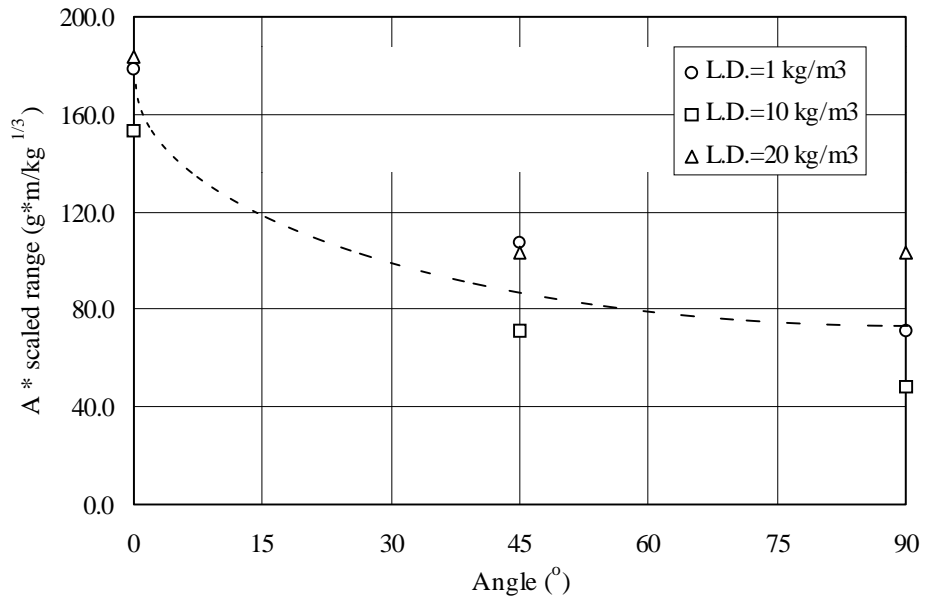


Figure 7. Normalized acceleration versus incident angle

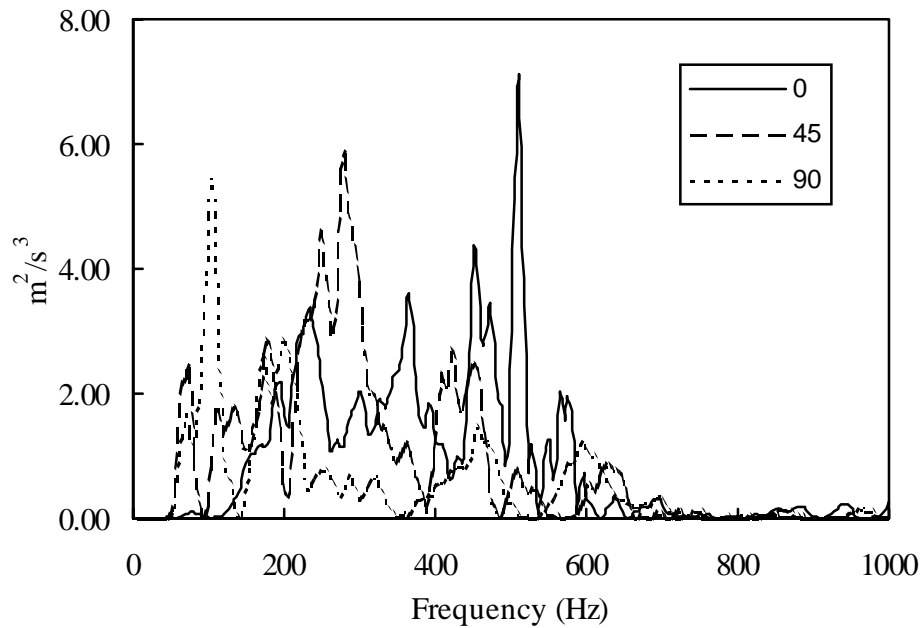


Figure 8. Power spectrum of shock waves at 0°, 45° and 90°

CONCLUSIONS

Through a series of small-scale tests, comprehensive data on ground shock propagation have been obtained for rock free field, rock surface, soil/rock interface, and soil surface. These data have allowed us to gain a better insight into the propagation of ground shock in mixed geological media and have been very useful in calibrating computer models.

The attenuation rates in rock derived from these tests seem to be low compared to tests conducted by WES and other larger tests. This may be due to the relatively small scale of these tests, where the rock is more likely to behave in the elastic range.

There are distinctive effects of the soil cover on ground shock propagation. At the same-scaled horizontal distance, ground shock in free field tends to be order of magnitude larger than on the soil surface, showing the damping effects of soil. The effects are more pronounced for accelerations than for peak particle velocities, and for motions in the horizontal direction than in the vertical direction. Near the charge, vertical motions on the soil surface may be higher than those in the rock free field at the same scaled range. This is due to more pronounced wave reflection at the free surface and wave amplification at the soil/rock boundary.

Water-coupled explosion produced ground shock effects similar to fully coupled explosion. The effects of contact and charge shape are only significant in near field and will diminish with increased distance from the charge. This implies that for practical design, their effects may be ignored without significant sacrifice in safety or economy.

ACKNOWLEDGEMENT

The authors acknowledge permission by the LEO management to publish this paper. The views and opinions expressed in this paper are those of the authors and do not necessarily represent those of the LEO management.

REFERENCES

Dowding, C.H. (1996). Construction Vibrations. Prentice Hall, 610 pp.

Wu, Y.K., Hao, H., Zhou, Y., and Chong, O.Y., (1998) Propagation characteristics of blast-induced shock waves in a jointed rock mass. *International Journal of Soil Dynamics and Earthquake Engineering*. (accepted)